the IBM 370/168 computer using a minimum basis set of Slater orbitals (STO-3G). The program used for these ab initio calculations was Gaussian-80.[10]

Acknowledgment. T.P.F. and M.A.C. acknowledge support of this research by the National Science Foundation (Grant 81-09403). We thank Dr. Roger DeKock for helpful discussions, Dr. Daniel Chipman of the University of Notre Dame Radiation Laboratory for assistance with computer programming, and the Computer Center of the University of Notre Dame for computing time.

Contribution from the Department of Chemistry,
California State University, Los Angeles, California 90032

Correlation of Experimentally Obtained Isomer Stability Data with MNDO and ab Initio MO Calculations for *closo*-2,4-Dicarbaheptaborane Derivative Isomer Sets

Thomas Onak,* Eileen O'Gorman, Tereso Banuelos, Catherine Alfonso, and Marian Yu

Received January 30, 1989

Experimentally determined stabilities among certain *closo*-2,4-$C_2B_5H_7$ derivatives in various isomer sets are correlated to results obtained from the application of the MNDO semiempirical MO method and, in one isomer set, by the application of the Gaussian-86 ab initio method. Specifically, the stabilities for the carboranes *B*-X-*closo*-2,4-$C_2B_5H_6$ (X = Cl, Br, I, C_2H_5, $(CH_3)_3N^+$; 3 isomers each), *B,B'*-X_2-*closo*-2,4-$C_2B_5H_5$ (X = Br, I, C_2H_5; 5 isomers each), *B*-Cl-*B',B''*-$(C_2H_5)_2$-*closo*-2,4-$C_2B_5H_4$ (11 isomers), and *B,B'*-(*closo*-2,4-$C_2B_5H_6)_2$ (6 isomers) are considered.

Introduction

Recently we have applied the MNDO[1] semiempirical MO method to various boron-substituted methyl, chloro, and chloromethyl derivatives of *closo*-2,4-$C_2B_5H_7$.[2] Although small energy differences between isomers in each isomer set are found, the MNDO order of stabilities within various isomers sets, in general, parallels experimental observations. Access to a newer version of MNDO that contains the parameters for many of the higher elements has made it possible to extend this work to various bromo and iodo derivatives of $C_2B_5H_7$. Also, experimental stability data for *B*-X and *B,B'*-X_2 (X = Br, I) derivatives of *closo*-2,4-$C_2B_5H_7$ are available[3] for comparison to the calculated stabilities. Additionally, because experimental stability data on chlorodiethyl and mono- and diethyl derivatives of this same carborane,[4] as well as on coupled C_2B_5 compounds (*B,B'*-$(C_2B_5H_6)_2$)[5] and on *B*-$(CH_3)_3N^+$ derivatives,[6] are also published, it is convenient to include MNDO calculations on these in an effort to complete a comparison of MNDO isomer stabilities with all *closo*-dicarbaheptaborane isomer sets in which (relative) experimental stabilities have been assessed.

It is also desirable to see if ab initio calculations, employing the readily available Gaussian-86 program, could predict relative isomer stabilities. Unfortunately, Gaussian-86 calculational time needed for most all compounds mentioned in the present work would be prohibitive. Sufficient CPU time was available, however, to allow ab initio stability comparisons at reasonably high basis set levels to be made for the three *B*-Cl-*closo*-2,4-$C_2B_5H_6$ isomers.

Experimental Section

The MNDO semiempirical calculations were performed by employing MOPAC,[1,7] version 3.11, available for our use on the Cray X-MP/48 at the San Diego Supercomputer Center through the consortium at San Diego State University and on the SCS-40 computer situated at California State University, Sacramento, CA. The general approach that was used in finding a closo-geometry stationary point on the potential surface for each *closo*-$C_2B_5H_7$ derivative (atom labeling and the structure of the parent *closo*-2,4-$C_2B_5H_7$ and derivatives are illustrated in Figure 1) was as follows: (a) the geometry of the parent carborane, *closo*-2,4-$C_2B_5H_7$,[8] was modified by replacing the appropriate boron-bonded hydrogen(s) with substituents(s) directed along the former B-H bond spatial vectors; (b) initial guess bond distances (in pm) were 177 for B-Cl, 187 for B-Br, 202 for B-I, 167 for B-N, 157 for *exo*-B-C, and 162 for *exo*-B-B; (c) the initial geometry input for MNDO energy optimization was subject only to (parent) cage symmetry constraints as well as enforced planar configuration of the equatorial 2,3,4,5,6-CBCBB plane of the pentagonal bipyramidal carborane cage (Figure 1); (d) the MNDO output geometry from operation *c* was then input for further MNDO optimization, this time with no symmetry or other geometry restrictions (i.e., full optimization). In all but two cases, no difficulty was encountered in finding a *closo*-C_2B_5 stationary point geometry for each isomer that was nearly identical with that obtained with symmetry restrictions imposed. In those two instances, the 3-Cl-5,6-$(C_2H_5)_2$ and 3-Cl-1,5-$(C_2H_5)_2$ derivatives, application of the (c) → (d) approach resulted in a classical norbornane type of structure for the cage atoms (note: the MNDO norbornane structure was some 27.5 kcal/mol more stable than the corresponding closo framework). An additional approach was then implemented in an attempt to find a stationary point corresponding to a closo-cage structure. For both of these isomers the MNDO output geometry from a C(2)-B(3)-C(4)-B(5)-B(6) pentagonal planar-enforced (bipyramidal) molecule was utilized as the closo input geometry for further optimization (with all geometry restrictions released). A stationary point closo (pentagonal pyramidal) geometry was then found for both compounds. In all instances, the geometry-optimized output and consequent heat of formation obtained from operation d (labelled "total optimization" in the Figures) was very close to that obtained from operation c. For both the 3-Cl-5,6-$(C_2H_5)_2$ and 3-Cl-1,5-$(C_2H_5)_2$ derivatives, the MNDO-optimized pentagonal planar-enforced geometries and consequent heats of formation

(1) (a) Dewar, M. J. S.; McKee, M. L. *J. Am. Chem. Soc.* **1977**, *99*, 5231-5241. (b) Dewar, M. J. S.; McKee, M. L. *Inorg. Chem.* **1980**, *19*, 2662-2672. (c) Dewar, M. J. S.; Thiel, W. *J. Am. Chem. Soc.* **1977**, *99*, 4899-4907. (d) Dewar, M. J. S.; Thiel, W. *J. Am. Chem. Soc.* **1977**, *99*, 4907-4917. (e) Dewar, M. J. S.; McKee, M. L. *J. Am. Chem. Soc.* **1978**, *17*, 1569-1581.
(2) O'Gorman, E.; Banuelos, T.; Onak, T. *Inorg. Chem.* **1988**, *27*, 912-915.
(3) Ng, B.; Onak, T.; Banuelos, T.; Gomez, F.; DiStefano, E. W. *Inorg. Chem.* **1985**, *24*, 4091-4096.
(4) Nam, W.; Abdou, Z. J.; Lee, H.; Banuelos, T.; Onak, T. *Inorg. Chem.* **1989**, *28*, 669-675.
(5) (a) Plotkin, J. S.; Astheimer, R. J.; Sneddon, L. G. *J. Am. Chem. Soc.* **1979**, *101*, 4155-4163. (b) Also, see ref 15 in ref 5a: Williams, R. E.; Gerhart, F. J.; Hickey, G. I.; Ditter, J. F. *U. S. C. F. S. T. I., AD Rep.* **1969**, *No. 693314*.
(6) Siwapinyoyos, G.; Onak, T. *Inorg. Chem.* **1982**, *21*, 156-163; *J. Am. Chem. Soc.* **1980**, *102*, 420.
(7) Stewart, J. J. P. *Quantum Chem. Program Exch. Bull.* **1986**, *6*, 99.
(8) (a) Beaudet, R. A.; Poynter, R. L. *J. Am. Chem. Soc.* **1964**, *86*, 1258-1259. (b) Beaudet, R. A.; Poynter, R. L. *J. Chem. Phys.* **1965**, *43*, 2166-2170. (c) Onak, T.; Dunks, G. B.; Beaudet, R. A.; Poynter, R. L. *J. Am. Chem. Soc.* **1966**, *88*, 4622-4625. (d) McNeill, E. A.; Scholer, F. R. *J. Mol. Struct.* **1975**, *27*, 151-159.

0020-1669/90/1329-0335$02.50/0

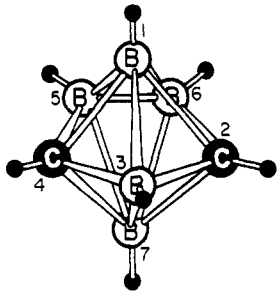

Figure 1. Ball and stick model and cage numbering of the parent *closo*-2,4-$C_2B_5H_7$.

Table I. MNDO Heats of Formation for Monobromo- and Dibromo and Monoiodo and Diiodo Derivatives of $C_2B_5H_7$

	ΔH_f, kJ	
compd	TO[a]	S/E[a]
1-Br	108.102	108.127
3-Br	100.788	100.788
5-Br	104.859	104.859
1,3-Br_2	67.877	67.902
1,5-Br_2	72.266	72.286
1,7-Br_2	77.550	77.550
3,5-Br_2	65.442	65.442
5,6-Br_2	69.555	69.555
1-I	144.302	144.331
3-I	139.725	139.725
5-I	137.034	137.034
1,3-I_2	142.570	142.603
1,5-I_2	139.630	139.670
1,7-I_2	147.917	147.917
3,5-I_2	136.352	136.352
5,6-I_2	132.424	132.424

[a] The TO cited heats of formation (column 2) are the result of a total MNDO geometry optimization of the closo pentagonal-bipyramidal framework (i.e. a closo-geometry stationary point found by removing all symmetry and other geometry restrictions after an initial S/E optimization); the S/E values are obtained by placing symmetry and equatorial C_2B_3 constraints on the molecule before carrying out the optimization procedure.[2]

Table II. Heats of Formation (MNDO) and Ethyl/Cage Dihedral Angles for *B*-Ethyl and *B,B'*-Diethyl Derivatives of *closo*-2,4-$C_2B_5H_7$

compd	ΔH_f,[a] kJ	dihedral Et-B(*X*)-B(*Y*), deg (*X,Y;Z*)[b]
1-Et-2,4-$C_2B_5H_6$	63.183	101 (1,3;2)
3-Et-2,4-$C_2B_5H_6$	59.224	0 (3,1)
5-Et-2,4-$C_2B_5H_6$	64.224	9 (5,1;4)
1,3-Et_2-2,4-$C_2B_5H_5$	−18.000	100 (1,3;2)
		1 (3,7;2)
1,5-Et_2-2,4-$C_2B_5H_5$	−13.159	101 (1,3;2)
		9 (5,7;4)
1,7-Et_2-2,4-$C_2B_5H_5$	−14.711	101 (1,3;2)
		101 (7,3;4)
3,5-Et_2-2,4-$C_2B_5H_5$	−17.962	0 (3,1)
		6 (5,7;4)
5,6-Et_2-2,4-$C_2B_5H_5$	−10.519	4 (5,1;4)
		4 (6,7;2)

[a] The cited heats of formation are the result of a total MNDO geometry optimization of the closo pentagonal-bipyramidal framework and the attached ethyl group(s); see footnote *a* of Table I. [b] Definition of (*X,Y;Z*): the dihedral Et-B(*X*)-B(*Y*) angle is measured about the bond between boron atom *X* and the methylene carbon of the ethyl group; if the angle is more than 0° the ethyl group is slanting toward cage atom *Z*. Each cited dihedral Et-B-B angle represents the lowest energy ethyl (rotational) position on the MNDO energy scale.

Table III. Heats of Formation (MNDO) and Ethyl/Cage Dihedral Angles for *B*-Chloro-*B',B''*-diethyl Isomer Derivatives of *closo*-2,4-$C_2B_5H_7$

compd	ΔH_f,[a] kJ	dihedral Et-B(*X*)-B(*Y*), deg (*X,Y;Z*)[b]
1-Cl-3,5-Et_2-2,4-$C_2B_5H_4$	−115.014	1 (3,1;2)
		4 (5,7;2)
1-Cl-3,7-Et_2-2,4-$C_2B_5H_4$	−113.558	1 (3,1;2)
		101 (7,3;2)
1-Cl-5,6-Et_2-2,4-$C_2B_5H_4$	−107.822	7 (5,1;4)
		5 (6,7;2)
1-Cl-5,7-Et_2-2,4-$C_2B_5H_4$	−109.031	9 (5,1;4)
		101 (7,3;2)
3-Cl-1,5-Et_2-2,4-$C_2B_5H_4$	−119.365	100 (1,3;2)
		10 (5,7;4)
3-Cl-1,7-Et_2-2,4-$C_2B_5H_4$	−121.754	101 (1,3;2)
		101 (7,3;4)
3-Cl-5,6-Et_2-2,4-$C_2B_5H_4$	−116.378	5 (5,1;4)
		5 (6,7;2)
5-Cl-1,3-Et_2-2,4-$C_2B_5H_4$	−117.964	100 (1,3;2)
		3 (3,7;4)
5-Cl-1,6-Et_2-2,4-$C_2B_5H_4$	−112.888	80 (1,3;4)
		1 (6,7;2)
5-Cl-1,7-Et_2-2,4-$C_2B_5H_4$	−115.114	100 (1,3;2)
		90 (7,3;4)
5-Cl-3,6-Et_2-2,4-$C_2B_5H_4$	−117.374	1 (3,1;2)
		1 (6,7;2)

[a] The cited heats of formation are the result of a total MNDO geometry optimization of the closo pentagonal-bipyramidal framework and the attached ethyl group(s). [b] Definition of (*X,Y;Z*): the dihedral Et-B(*X*)-B(*Y*) angle is measured about the bond between boron atom *X* and the methylene carbon of the ethyl group; if the angle is more than 0° the ethyl group is slanting toward cage atom *Z*. Each cited dihedral Et-B-B angle represents the lowest energy ethyl (rotational) position on the MNDO energy scale.

were very nearly those obtained from the subsequent optimization in which all geometry restrictions were released. The results for the *B*-X (X = Br, I, C_2H_5; 3 isomers apiece), the *B,B'*-X_2 (X = Br, I, C_2H_5; 5 isomers apiece), and *B*-Cl-*B',B''*-$(C_2H_5)_2$ compounds (11 isomers) are given in Tables I–III and Figures 2–4.

In the case of the C_2H_5 and $(CH_3)_3N$ derivatives of *closo*-2,4-$C_2B_5H_7$, as well as the coupled carborane isomer set, it was necessary to carry out many calculations for each compound in which the appended group onto the carborane cage was subjected to a series of appropriate rotations in order to locate the most stable conformation of the substituent.

MNDO calculations of *B,B'*-$(C_2B_5H_6)_2$ with varying *exo*-B-B twist angles give a result for the equatorially bonded B-B isomers that is reminiscent of that found for 2,2'-[*closo*-1,5-$C_2B_3H_4]_2$.[9] For each of the six coupled *B,B'*-$(C_2B_5H_6)_2$ carboranes, the MNDO energy preferred conformations are shown in Figure 5. For the three isomers, 3,3'-, 3,5'-, and 5,5'-(*closo*-2,4-$C_2B_5H_6)_2$, the equatorial C_2B_3 planes are at, or not far from, right angles to each other (i.e. 90° for C(2)B(3)B(3')C(2') of 3,3'-(*closo*-2,4-$C_2B_5H_6)_2$, 90° for C(2)B(3)B(5')C(4') of 3,5'-(*closo*-2,4-$C_2B_5H_6)_2$, and 103° for C(4)B(5)B(5')C(4') of 5,5'-(*closo*-2,4-$C_2B_5H_6)_2$). A number of MNDO calculations carried out upon varying the *exo*-B-B twist angle revealed that the least stable conformation was located when the two equatorial C_2B_3 sets were in, or nearly in, the same plane. In the 3,3'-isomer the energy difference between the most and least stable rotamers was 4.05 kJ/mol; in the 3,5'-isomer, 3.97 kJ/mol; in the 5,5'-isomer, 6.27 kJ/mol. For the 1,3'- and 1,5'-isomers the equatorial plane of the primed carborane cage prefers to be not far from 90° relative to the other cage's B(1)-B(3)-B(7) plane. In the case of the 1,3'-isomer, the angle is 91°, and in the case of the 1,5'-isomer, the energy-preferred dihedral angle is 99°; the least stable conformers are found at twist angles of close to 0° with an energy change of ca. 3.7 kJ/mol for the 1,3'-isomer and ca. 2.9 kJ/mol for the 1,5'-isomer (as compared to the most stable conformation). In the case of the 1,1'-isomer, the preferred B(3)B(1)B(1')B(3') twist angle is 108°; the least stable conformation is found at a twist angle close to 90° from the most stable conformation, and the energy difference between the most stable and least stable twist angle conformers is ca. 2.5 kJ/mol. Fully geom-

(9) Anderson, E. L.; DeKock, R. L.; Fehlner, T. P. *J. Am. Chem. Soc.* **1980**, *102*, 2644–2650.

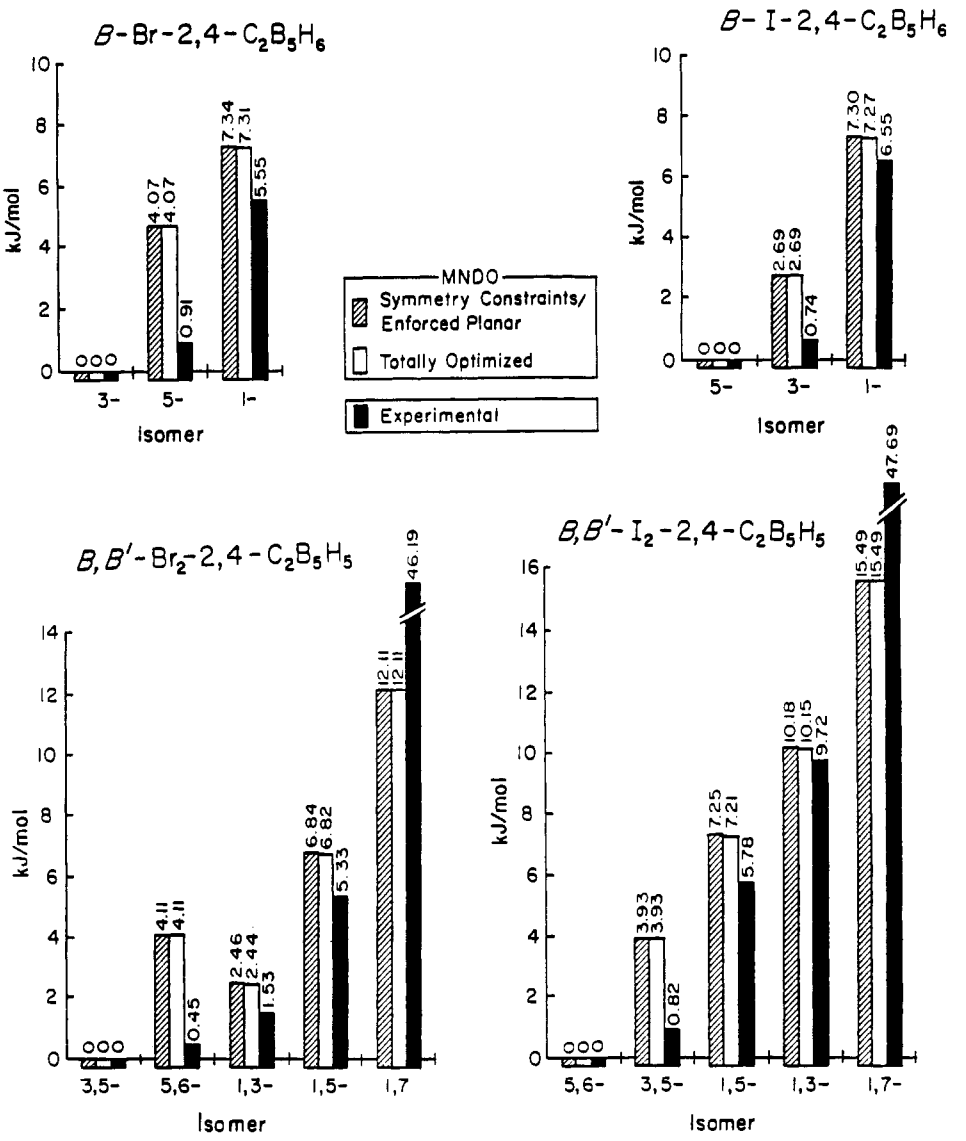

Figure 2. Bar graph comparison of the (relative) MNDO-derived enthalpies (Table I, columns 2 and 3) with experimental values[3] for each of the three-isomer sets *B*-X-2,4-$C_2B_5H_6$ (X = Br, I) and for each of the five-isomer sets *B,B'*-X_2-2,4-$C_2B_5H_5$ (X = Br, I). The isomer with the lowest enthalpy in each set is arbitrarily assigned a base value of $\Delta H = 0$.

Table IV. Calculated ab Initio Energies[a] of the Three *B*-Cl-*closo*-2,4-$C_2B_5H_6$ Isomers

calculational level[b]	energy		
	1-Cl-$C_2B_5H_6$	3-Cl-$C_2B_5H_6$	5-Cl-$C_2B_5H_6$
HF/STO-3G OPT	−654.834 567 6	−654.837 137 9	−654.837 527 1
HF/3-21G OPT	−658.844 134 9	−658.848 375 7	−658.848 414 1
HF/6-31G OPT	−662.057 103 0	−662.061 670 9	−662.061 668 2
6-31G*//6-31G	−662.187 265 2	−662.190 645 9	−662.189 864 4
CID/6-31G// 6-31G	−662.522 209 7	−662.526 272 2	−662.525 866 1
CID/6-31G*// 6-31G	−662.878 571 5	−662.881 090 6	−662.880 152 7
MP3/6-31G*// 6-31G	−663.050 659 4	−663.053 040 3	−663.051 880 8

[a] In au. [b] Geometry optimization on the last basis set cited; e.g. CID/6-31G*//6-31G is defined as a CID/6-31G* single-point calculation on a 6-31G optimized geometry.[12]

etry-optimized *B,B'*-$(C_2B_5H_6)_2$ isomers having the energy-preferred *exo-B,B'* cage twist angles cited above and depicted in Figure 5 are associated with the following MNDO ΔH_f values (in kcal/mol): 66.372 for the 1,1'-isomer; 66.761 for the 1,3'-isomer; 66.282 for the 1,5'-isomer; 67.510 for the 3,3'-isomer; 67.007 for the 3,5'-isomer 66.914 for the 5,5'-isomer.

In all of the MNDO optimizations the PRECISE command option was turned on.[10] All calculations reached SCF convergence; most satisfied Herbert's test; for the remaining, further work was not justified because of the shallowness of the energy gradient.[10]

Ab initio SCF MO calculations on the three *B*-Cl-*closo*-2,4-$C_2B_5H_6$ isomers were carried out by using a Gaussian-86 program[11,12] on, variously, the computers cited at the top of the experimental section or on an ELXSI computer in the California State University Central Computing Facility. (Note: a few Gaussian-86 benchmark calculations on each of the computers showed the Cray X-MP/48 to be about 3 to 5 times faster than the SCS-40 and the latter to be about 2.5–4 times faster than the ELXSI; also, it took slightly more than 50 h of SCS-40 CPU time to run a 6-31G* OPT calculation on the 5-Cl-2,4-$C_2B_5H_6$ geometry from the 6-31G fully optimized geometry.) Input geometry for the Gaussian-86 STO-3G optimizations were obtained from the MNDO-optimized output geometries. Subsequently, the STO-3G geometry optimized output was used for the 3-21G optimization, etc., until the 6-31G optimized geometry was obtained. Thereafter, the CID/6-31G* and MP3/6-31G* energies (Table IV) were obtained as single-point calcu-

(10) Boyd, D. B.; Smith, D. W.; Stewart, J. J. P.; Wimmer, E. *J. Comput. Chem.* **1988**, *9*, 387–398.
(11) Frisch, M. J.; Binkley, J. S.; Schlegel, H. B.; Raghavachari, K.; Melius, C. F.; Martin, R. L.; Stewart, J. J. P.; Bobrowisz, F. W.; Rohlfing, C. M.; Kahn, L. R.; Defrees, D. J.; Seeger, R.; Whiteside, R. A.; Fox, D. J.; Fleuder, E. M.; Pople, J. A. "Gaussian-86"; Carnegie-Mellon Quantum Chemistry Publishing Unit: Pittsburgh, PA, 1984.
(12) Hehre, W. J.; Radon, L.; Schleyer, P. v. R.; Pople, J. A. *Ab Initio Molecular Orbital Theory*; Wiley-Interscience: New York, 1986.

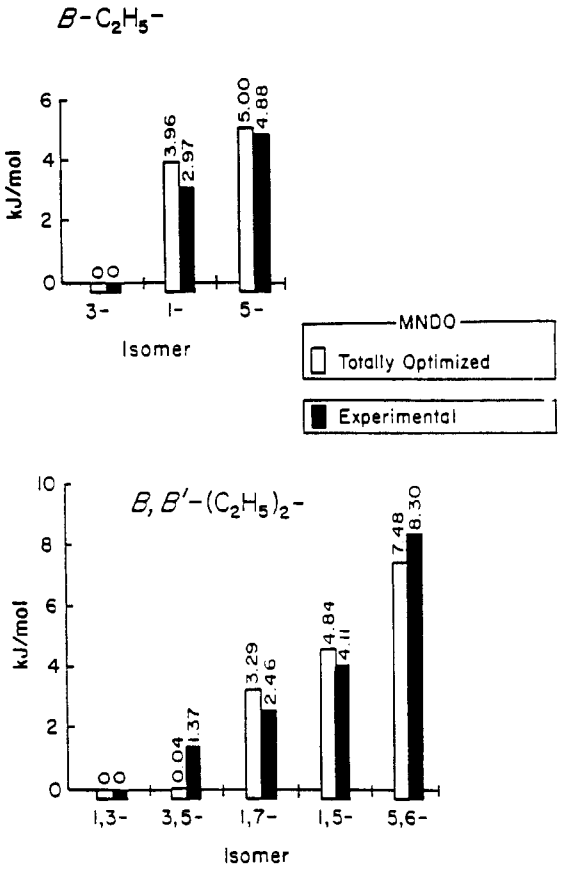

Figure 3. bar graph comparison of the relative MNDO-derived enthalpies (Table II) with experimental values[4] for the three *B*-monoethyl and the five *B,B'*-diethyl isomers of *closo*-2,4-$C_2B_5H_7$. The isomer with the lowest enthalpy in each set is arbitrarily assigned a base value of $\Delta H = 0$.

lations on the higher quality 6-31G basis set optimized geometry. As previously noted[12,13] CID/6-31G*//6-31G implies a single-point CID/6-31G* calculation for an optimized 6-31G structure. The three *R*-Cl-*closo*-2,4-$C_2B_5H_6$ isomers were geometry optimized within their respective point groups.

Results and Discussion

***B*-Bromo and *B*-Iodo Derivatives.** Experimentally derived isomer enthalpy differences for various *B*-X and *B,B'*-X_2 (X = Br, I) derivatives of *closo*-2,4-$C_2B_5H_7$[3] are compared to MNDO-calculated (relative) heats of formation (Table I, column 3) in Figure 2. Except for one minor departure, cf. the 5,6- and 1,3-isomers of *B,B'*-Br_2-2,4-$C_2B_5H_5$, parallel isomer stabilities are found within all isomer sets. Specifically, both the MNDO and experimental results show the following isomer stability order among the mono- and disubstituted *closo*-$C_2B_5H_7$ compounds *B*-X-*closo*-2,4-$C_2B_5H_6$ (three isomers for each X), and *B,B'*-X_2-*closo*-2,4-$C_2B_5H_5$ (X = Br, I; five isomers each):

B-monobromo: 3 > 5 > 1 (exptl and MNDO)

B-monoiodo: 5 > 3 > 1 (exptl and MNDO)

B,B'-dibromo: 3,5 > 5,6 > 1,3 > 1,5 > 1,7 (exptl)

B,B'-dibromo: 3,5 > 1,3 > 5,6 > 1,5 > 1,7 (MNDO)

B,B'-diiodo: 5,6 > 3,5 > 1,5 > 1,3 > 1,7 (exptl and MNDO)

***B*-Ethyl, *B,B'*-Diethyl, and *B*-Chloro-*B',B''*-diethyl Derivatives.** Both the MNDO (present work) and experimental results[4] show the following isomer stability order among the B-mono- and B,B'-disubstituted *B*-ethyl *closo*-$C_2B_5H_7$ derivatives (Table II, Figure 3):

B-monoethyl: 3 > 1 > 5 (exptl and MNDO)

B,B'-diethyl:

1,3 > 3,5 > 1,7 > 1,5 > 5,6 (exptl and MNDO)

This order of stability is similar to that found for the corresponding methyl derivatives.[14]

Of the 11 *B*-chloro-*B',B''*-diethyl-substituted isomers of *closo*-2,4-$C_2B_5H_7$,[4] MNDO predicts very well the most (3,1,7) and the least (1,5,6) stable of the isomers but does not predict as well the order for the intermediate-stability isomers, e.g. 5-Cl-1,6-$(C_2H_5)_2C_2B_5H_4$ (Table III, Figure 4).

exptl (Cl, C_2H_5, C_2H_5): 3,1,7 = 5,1,3 > 5,3,6 > 3,1,5 > 5,1,7 > 5,1,6 > 1,3,5 > 3,5,6 > 1,3,7 = 1,5,7 > 1,5,6

MNDO (Cl, C_2H_5, C_2H_5): 3,1,7 > 3,1,5 > 5,1,3 > 5,3,6 > 3,5,6 > 5,1,7 > 1,3,5 > 1,3,7 > 5,1,6 > 1,5,7 > 1,5,6

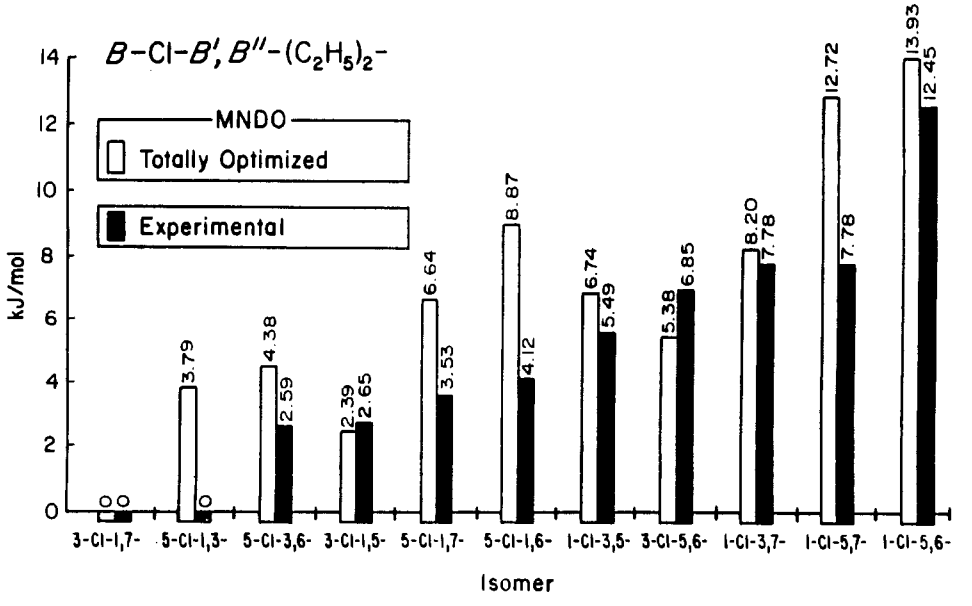

Figure 4. Bar graph comparison of the relative MNDO-derived enthalpies (Table III) with experimental values[4] for the eleven *B*-monochloro-*B',B''*-diethyl isomers of *closo*-2,4-$C_2B_5H_7$. The isomer with the lowest enthalpy in the set is arbitrarily assigned a base value $\Delta H = 0$.

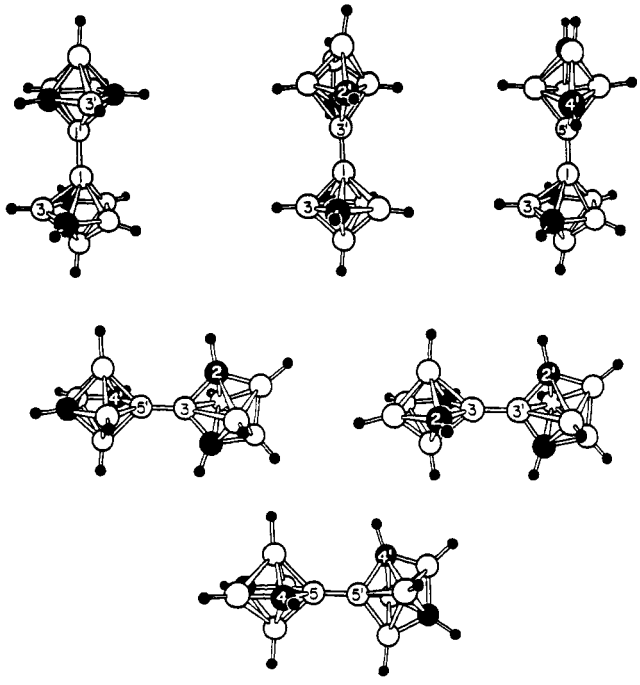

Figure 5. MNDO-favored conformations of each of the six *B,B'*-(2,4-$C_2B_5H_6)_2$ isomers (see text for cage–cage twist angle values).

***B*-$(CH_3)_3N^+$ Derivatives.** The relative (geometry-optimized) MNDO stabilities of the three *B*-$(CH_3)_3N^+$ derivatives of *closo*-2,4-$C_2B_5H_7$ are 5 > 3 > 1 (e.g. MNDO ΔH_f (kcal): +212.738 for the 5-isomer, +215.400 for the 3-isomer, and +218.207 for the 1-isomer). The only experimental indication of the relative stabilities of this set of isomeric compounds comes from the products observed upon reaction of trimethylamine with the three *B*-Cl-*closo*-2,4-$C_2B_5H_6$ isomers. Removal of the chlorine, as chloride ion, from the consequent amine adducts gives rise to the *B*-$(CH_3)_3N^+$ derivatives. Both the 5-chloro- and 3-chloro-carboranes yield the respective 5- and 3-$(CH_3)_3N^+$ derivatives. However, the 1-chloro system (in chloroform solvent) gives only the 3-$(CH_3)_3N^+$ isomer.[6] This rearrangement can be interpreted as an indication of greater 3-isomer stability (as compared to the 1-isomer). It is satisfying to know that a simple consideration of MNDO stabilities does predict the correct stability order for the 1- and the 3-isomers although solvent effects are necessarily neglected in the MNDO calculation.

$(C_2B_5H_6)_2$. From equilibration studies[5] it has been stated that, within experimental error (as high as 28% in one instance), the relative stabilities of the six *B,B'*-$(C_2B_5H_6)_2$ isomers are about the same; i.e., approximately statistical quantities (a ratio of 4:4:8:1:4:4 for the 1,1'-, 1,3'-, 1,5'-, 3,3'-, 3,5'-, and 5,5'-isomers) are found under thermal rearrangement conditions. If exactly statistical quantities were found, this would imply, of course, that enthalpy differences between isomers are zero. An examination of the relative MNDO ΔH_f values for the *B,B'*-$(C_2B_5H_6)_2$ isomer series gives the stability order 1,5' > 1,1' > 1,3' > 5,5' > 3,5' > 3.3'. It is interesting to note that if the measured departures[5] from statistical quantities are used as indicators of relative stabilities, then one finds experimentally the following order: 3,5' > 1,5' > 5,5' > 1,1' > 1,3' > 3,3'. In both cases (MNDO and experimental) four of the six isomers follow the same stability pattern—1,5' > 1,1' > 1,3' > 3,3'—and the 5,5'-isomer is close to the middle of both sequences. Only the 3,5'-isomer appears to be much out of order and predicted to be less stable by MNDO than found experimentally. It is to be noted, though, that the 3,5'-isomer was the starting isomer in the thermal rearrangement[5] from which the equilibration results were obtained, so it is tempting to suggest that not all of the 3,5'-isomer had sufficient time to equilibrate with the remaining isomers. It would be of some interest to repeat the thermal rearrangement, and equilibration, but by starting with an isomer other than the 3,5'-isomer.

The MNDO fully optimized structures of the six *B,B'*-(*closo*-2,4-$C_2B_5H_6)_2$ isomers are given in Figure 5. The cage–cage conformations of many of these (3,3', 3,5', and 5,5) are reminiscent of those found for 2,2'-(1,5-$C_2B_3H_4)_2$ and 2,2'-3,2'-(1,5-$C_2B_3H_4)_2$-1,5-$C_2B_3H_3$ in which a π-type interaction across the exopolyhedral B–B bond has been suggested.[9]

Gaussian-86 Calculations on *B*-Cl-*closo*-2,4-$C_2B_5H_6$ Isomers. Ab initio calculations on the three *B*-Cl-*closo*-2,4-$C_2B_5H_6$ isomers at the Gaussian-86 STO-3G level confirm that the wrong order of stability is predicted, by using this basis set, for the 3- and the 5-isomers.[15] We find that this incorrect order of stabilities continues at the 3-21G level but begins to turn around at the 6-31G level (Table IV, Figure 6). However, as the quality of the basis set is increased to this point, the 1-isomer, although continuing to be the least stable during this series of calculations, shifts to relative energy values that are increasingly disparate. Adding configuration interaction with douuble substitutions shifts the relative energy values closer to those experimentally observed, but a better correspondence to the experimental[16] relative ΔH values is experienced upon incorporating d orbitals for the non-hydrogen atoms (i.e. 6-31G* level). At the CID/6-31G*//6-31G and MP3/6-31G*//6-31G levels, the calculated relative enthalpies are almost those, within experimental error, assessed by experimental equilibration results.[16]

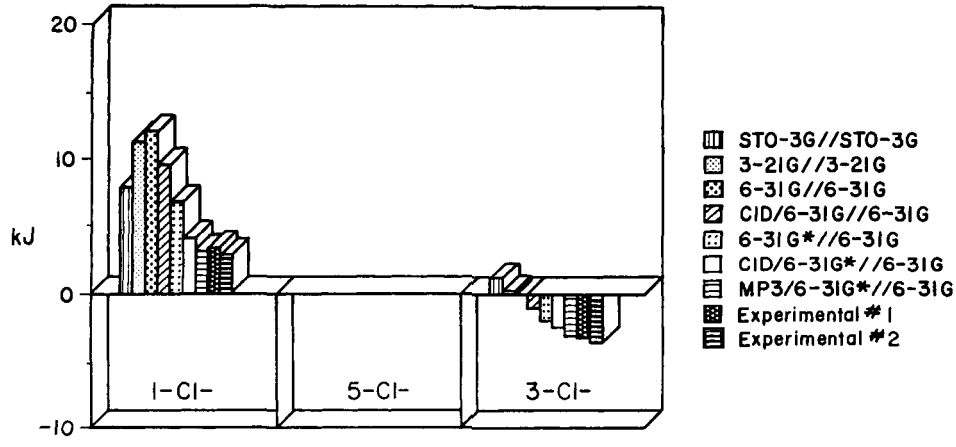

Figure 6. Bar graph comparison of the Gaussian-86-derived relative enthalpies, in kJ, of the three *B*-Cl-*closo*-2,4-$C_2B_5H_6$ isomers obtained while varying the orbital basis set (see Table IV). The energy value for the 5-Cl isomer is arbitrarily set to zero in each case. The relative experimental energies are obtained from two sources.[16b,c]

These results could well suggest that all future ab initio calculations on substituted carboranes be conducted at least to the CID/6-31G*//6-31G or MP3/6-31G*//6-31G level for useful information about relative stabilities. Unfortunately, this is not practical for the other derivatives discussed herein because of computer time constraints, especially upon considering that many (e.g., ethyl and trimethylamino) rotamer possibilities would need examination.

Acknowledgment. We wish to thank the National Science Foundation, Grant CHE-8617068, and the MBRS-NIH program (T.B., C.A.) for partial support of this study. We also thank San Diego State University for access to the San Diego Supercomputer Regional Facility and California State University, Sacramento, CA, for access to the SCS-40 and Multiflow Trace (NSF Grant CHE-8822716) minisupercomputer facilities.

(13) Clark, T. *Computational Chemistry*; Wiley-Interscience: New York, 1985.
(14) (a) Oh, B.; Onak, T. *Inorg. Chem.* **1982**, *21*, 3150-3154. (b) Onak, T.; Fung, A. P.; Siwanpinyoyos, G.; Leach, J. B. *Inorg. Chem.* **1979**, *18*, 2878-2882.
(15) Beltram, G. A.; Jasperse, C.; Cavanaugh, M. A.; Fehlner, T. P. *Inorg. Chem.*, preceding paper in this issue.
(16) (a) Takimoto, C.; Siwapinyoyos, G.; Fuller, K.; Fung, A. P.; Liauw, L.; Jarvis, W.; Millhauser, G.; Onak, T. *Inorg. Chem.* **1980**, *19*, 107-110. (b) Abdou, Z. J.; Soltis, M.; Oh, B.; Siwap, G.; Banuelos, T.; Nam, W.; Onak, T. *Inorg. Chem.* **1985**, *19*, 2363-2367. (c) Abdou, Z. A.; Abdou, G.; Onak, T.; Lee, S. *Inorg. Chem.* **1986**, *25*, 2678-2683.

Contribution from the Department of Chemistry and Saskatchewan Accelerator Laboratory, University of Saskatchewan, Saskatoon, SK, Canada S7N 0W0, and Bereich Strahlenchemie, Hahn-Meitner-Institut Berlin GmbH, Postfach 39 01 28, D-1000 Berlin 39, Federal Republic of Germany

Radiolytic Study of the Reactions of Hydroxyl Radical with Cobalt(III), Iron(II), and Ruthenium(II) Complexes Containing 2,2'-Bipyridyl and Cyano Ligands

A. C. Maliyackel,[1a] W. L. Waltz,*[1a] J. Lilie,[1b] and R. J. Woods[1a]

Received July 3, 1989

The reactions of hydroxyl radical with the complex ions $[Co(bpy)_3]^{3+}$, $[Fe(bpy)_3]^{2+}$, $[Fe(bpy)_2(CN)_2]$, $[Fe(bpy)(CN)_4]^{2-}$, $[Fe(CN)_6]^{4-}$, $[Fe(Me_2bpy)_3]^{2+}$, and $[Ru(bpy)_3]^{2+}$ and with bpy and $Hbpy^+$, where bpy = 2,2'-bipyridine and Me_2bpy = 4,4'-dimethyl-2,2'-bipyridine, have been investigated in N_2O-saturated aqueous media. The results from time-resolved studies, carried out by using pulse radiolysis in conjunction with conductivity and near-UV-visible optical detection methods, show that the OH reactions occur with rate constants in the range $(2-17) \times 10^9$ M^{-1} s^{-1}. For the reactions of bpy and the tris(bipyridyl) complex ions, the absence of significant conductivity movements accompanying the initial optical changes demonstrates that the processes are ones involving OH addition to the systems. The products are reactive toward hexacyanoiron(III) and molecular oxygen, and the associated findings clearly implicate these species to be of a ligand-radical type; however, the evidence also indicates in several cases the occurrence of more than one initially observed product. The reaction of ferrocyanide involves electron transfer whereas for the mixed cyano-bipyridyl complexes of iron(II) both electron-transfer and OH-addition processes are encountered, and the predominant process for $[Fe(bpy)(CN)_4]^{2-}$ proceeds by an inner-sphere electron-transfer mechanism. Determinations for some of the final products arising from the pulse and γ-ray radiolysis of the mixed cyano-bipyridyl complexes, $[Co(bpy)_3]^{3+}$, and $[Fe(bpy)_3]^{2+}$ have been undertaken in order to obtain insight into the overall sequence of events, and the natures of the mechanisms are discussed.

Introduction

The hydroxyl radical is one of the strongest single-electron oxidizing agents ($E°(OH/OH^-)$ = 1.89 V) available for use in aqueous media to study oxidation-reduction processes.[2-4] While its occurrence is perhaps most often associated with radiolytic investigations where it is one of the primary products of water degradation, hydroxyl radical is encountered in many other contexts, notably those pertaining to photolysis, sonolysis, and thermal reactions such as the Fenton-type processes involving interactions of metal ions with hydrogen peroxide. Recent reviews indicate that studies of the OH reactions with inorganic substances, in particular metal complex ions, now number well into the several hundreds.[3,4] Because of the transitory existence of this free radical and the fact that it absorbs only weakly in the UV region, its reaction mechanisms with inorganic materials and the features that influence the processes are in many respects not clearly understood; however, hydroxyl radical does exhibit considerable diversity in its mechanistic behavior.

As one would expect for a single-electron oxidant, reactions of hydroxyl radical with metal complex ions are found that proceed in an overall sense by electron transfer as exemplified by its reaction with ferrocyanide (eq 1). Because of the perception that

$$[Fe(CN)_6]^{4-} + OH \rightarrow [Fe(CN)_6]^{3-} + OH^- \quad (1)$$

the transformation of OH(aq) to OH^-(aq) engenders considerable solvent reorganization, it has been proposed that electron-transfer processes such as that of eq 1 proceed via inner-sphere pathways rather than by outer-sphere ones.[4-6] In this context, the inner-sphere terminology is being used in a somewhat broader sense than the classical definition; namely, it is meant to imply that electron transfer is promoted by strong electronic interactions (chemical bond formation) as discussed by Linck.[7] Evidence for inner-sphere processes for OH reactions with metal complex ions has been generally circumstantial although results obtained by using conductivity detection for metal aquo ions clearly point to this, and recently the reaction of $[IrCl_6]^{3-}$ and OH to yield $[IrCl_6]^{2-}$ has been shown to involve two pathways, the major one entailing OH adduct formation.[4,8] In contrast, inner-sphere processes encompassing formation of adducts are commonly found in the interactions of OH with simple non-metal anions such as cyanide and chloride (eqs 2 and 3).[3,4,9]

$$Cl^- + OH \rightleftarrows ClOH^{\bullet -} \quad (2)$$

$$ClOH^{\bullet -} + H^+ \rightleftarrows Cl + H_2O \quad (3)$$

* To whom correspondence should be addressed.

(1) (a) University of Saskatchewan. (b) Hahn-Meitner-Institut Berlin GmbH.
(2) Schwarz, H. A.; Dodson, R. W. *J. Phys. Chem.* **1984**, *88*, 3643.
(3) Buxton, G. V.; Greenstock, C. L.; Helman, W. P.; Ross, A. B. *J. Phys. Chem. Ref. Data* **1988**, *17*, 513.
(4) Waltz, W. L. In *Photoinduced Electron Transfer*; Fox, M. A., Chanon, M., Eds.; Elsevier: Amsterdam, 1988; Part B, pp 57-109.
(5) Zehavi, D.; Rabani, J. *J. Phys. Chem.* **1972**, *76*, 3703.
(6) Lati, J.; Meyerstein, D. *J. Chem. Soc., Dalton Trans.* **1978**, 1105.
(7) Linck, R. G. In *Inorganic Reactions and Methods*; Zuckerman, J. J., Ed.; VCH Publishers: Deerfield Beach, FL, 1986; Vol. 15, pp 9-13.
(8) Selvarajan, N.; Raghavan, N. V. *J. Chem. Soc., Chem. Commun.* **1980**, 336.

0020-1669/90/1329-0340$02.50/0